The consequences of imperfect mixing in autocatalytic chemical and biological systems

Irving R. Epstein

When chemical reactions whose rate increases with the concentration of a product species are carried out in imperfectly mixed systems, a variety of complex behaviours can occur. These phenomena, which have relevance for biological processes as well, include chaotic and stochastic behaviour and selection of one final state over an equally probable alternative.

ONE of the great conceptual revolutions that has taken place in the physical and, to a lesser extent, the biological sciences in this century is the recognition that nonlinearity is ubuiquitous and that it has profound effects on the dynamics of a system[1]. Although linear systems, in which superposition principles and the intuitively pleasing notion that the whole is equal to the sum of its parts, are often susceptible to exact mathematical analysis, they constitute but a small fraction of the real world. More and more, particularly with recent advances in computational power, science deals with nonlinear systems that give rise to complex temporal oscillation, chaos and spatial pattern formation.

One point that has perhaps been underappreciated is the extent to which spatial inhomogeneities can interact with and amplify the temporal nonlinearities in an evolving system so as to yield new and important phenomena. In any system governed by a nonlinear rate law, a knowledge of the bulk or average concentrations is not sufficient to predict the average rate of the reaction. One must also know the spatial distribution of reacting material. The further the rate laws depart from linearity, the more drastically the behaviour of the system changes when the spatial distribution is modified.

In many chemical and biological systems undergoing reaction and diffusion in the absence of mixing, strikingly similar and rather beautiful patterns spontaneously develop. The time-dependent spiral and target patterns seen in the Belousov–Zhabotinsky reaction[2], in aggregating slime moulds[3] and in developing oocytes[4] have been the subject of much attention, as have the stationary patterns of spots or stripes predicted by Turing[5] as a mechanism for morphogenesis and recently found experimentally in simple chemical systems[6].

Here I focus on the dramatic effects of a different aspect of the interaction between temporal nonlinearity and spatial inhomogeneity, the behaviour of imperfectly mixed, autocatalytic systems. Imperfect mixing in autocatalytic systems can, for example, lead to chemical reactions that occur at seemingly random intervals, crystallization processes that yield sometimes all left-handed and sometimes all right-handed crystals, and reactions in which changing the rate at which a solution is stirred can cause a transition from a stationary, time-independent state to one of periodic or even chaotic oscillation. These phenomena have been studied thus far primarily in inorganic chemical media; but there are possible implications also for living systems.

Autocatalysis

Autocatalysis—the enhancement of the (absolute) rate of growth of a population as that population increases—is ubiquitous in biological systems. It is, in a sense, the essence of reproduction. As the Reverend Thomas Malthus recognized when he suggested that population tends to grow geometrically, the number of individuals born is, on average, proportional to the number in the population. This perceptive clergyman was also aware that there are limitations to population growth; he proposed[7] that the food supply grows only arithmetically. As an alternative, one might construct a model of population growth that includes a fixed carrying capacity K for the environment, so that the population $N(t)$ tends toward K as time $t \rightarrow \infty$

$$dN/dt = \beta N(1 - N/K) \quad (1)$$

where β represents the average *per capita* excess of the birth rate over the death rate. Equation (1) is the logistic equation, one of the simplest and most thoroughly studied models of population dynamics. It contains the crucial elements of interest here, autocatalysis (the first term on the right-hand side) and nonlinearity (the second term, proportional to N^2).

Autocatalysis occurs also in non-living systems, albeit less commonly. In chemical systems it can lead to explosion (analogous to "the population explosion") if, for example, an exothermic reaction with a rate that increases sharply with temperature is run in a closed vessel that does not permit the heat generated by the reaction to escape rapidly enough.

Autocatalytic chemical reactions, when coupled to other reactions that provide a negative feedback to control the proliferation of the autocatalytic species, can give rise to such complex behaviour as periodic oscillation or chemical chaos. In configurations open to the flow of matter and/or energy, such as stirred-tank reactors[8], autocatalytic chemical systems can support multiple stable states, leading to hysteresis as a control parameter is varied.

Bifurcations and mixing

In many studies of chemically reacting media the assumption is made that the system is "well mixed", that is, that the concentration of each species is uniform throughout the system. To bring about this presumed state of homogeneity, experimenters often employ mechanical agitation, for example, a magnetic stirrer that revolves at hundreds or thousands of revolutions per minute (r.p.m.). If the reactions under study are nonlinear, any major departure from the assumption of perfect mixing can have major dynamical consequences.

In fact, perfect mixing is almost never achieved in practice, and chemical engineers, who must deal with the consequences of imperfectly mixed reactors containing large quantities of nonlinearly reacting materials, have been aware of this situation for decades. Mixing is an extremely complicated phenomenon occurring on multiple length scales and timescales. Engineers speak of two aspects of mixing, macromixing and micromixing. Macromixing is the intermingling of packets of fluid, such as those that enter a flow reactor in different input streams, to achieve a composition that appears homogeneous if sampled on a macroscopic scale. Micromixing, which is far slower and more difficult to achieve, involves the segregation of a fluid in vortices and filaments at very short length scales. Although much pro-

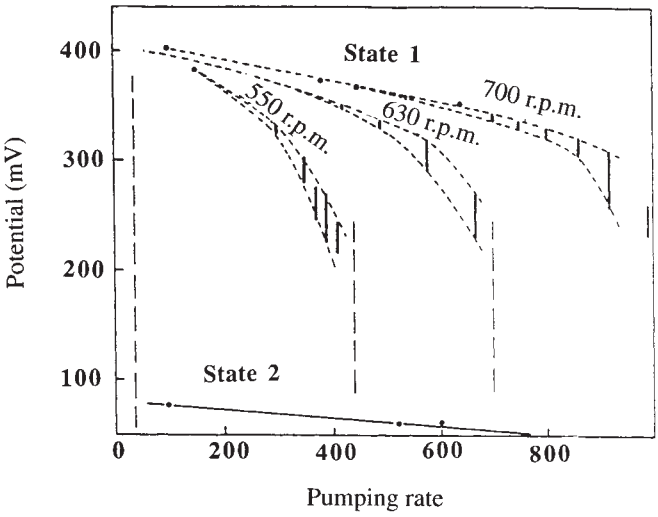

FIG. 1 Effects of stirring rate on bistability in the chlorite–iodide reaction[10]. Dashed line, steady-state potential in state I; solid line, steady-state potential in state II. Note how the bistable region shifts and broadens as the stirring rate is increased from 550 to 700 r.p.m. (The pumping rate is given in units of ~0.02 ml min^{-1}; the potential is that of a Pt electrode versus an $Hg/HgSO_4/K_2SO_4$ reference electrode.)

gress has been made toward understanding the factors that govern the degree of mixing in a system and toward developing reactor designs that improve the quality of mixing, particularly macromixing[9], the goal of a truly well-mixed system remains a distant one.

Rather than pursue the quest for the elusive (perhaps unattainable) grail of perfect mixing, it may be more useful to recognize the extent of imperfection that exists in systems of interest, and to assess the consequences that such imperfection brings.

One of the first demonstrations of the importance of mixing quality is found in a set of experiments by Roux *et al.*[10] on the chlorite–iodide reaction, a prototype system in nonlinear chemical dynamics[11], in a stirred-tank reactor. Typical results are shown in Fig. 1. Although the bistability and hysteresis in this system had previously been characterized both experimentally and theoretically, it came as a shock to most investigators that the critical flow rate for transition from the upper to the lower branch of steady states was strongly dependent on the stirring rate, even at relatively rapid rates. Luo and Epstein[12] later demonstrated that the stirring rate can be treated as a bifurcation parameter, like the flow rate or the input concentration of a reactant, which shifts the dynamical behaviour of the system among a series of steady and oscillatory states.

A simple model[13], illustrated in Fig. 2, provides a qualitative understanding of the origin of the phenomenon. Inevitably, some regions of the reactor, for example those closest to the stirrer, are better mixed than others. As the stirring rate increases, the relative size of the poorly mixed volume shrinks, although it never reaches zero. As a first approximation, we represent the actual reactor by two coupled reactors: one, the well-mixed region with volume V_a, in contact with the input and output flows; the other, the poorly mixed region with volume V_d, linked only to the well-mixed region but not to the external flows. The parameters Q_x (the cross-flow between V_a and V_d) and the ratio V_a/V_d are used to characterize the quality of the mixing, which improves as the stirring rate increases.

The originators of the model suggest that it is the ratio of the transition time between steady states of differing composition to the residence time in the reactor that determines how changing the degree of mixing will influence the stability of the two bistable branches of steady states. If the transition time (induction period) is relatively short, then poorly mixed regions will be found on the thermodynamic (low-flow-rate) branch, that is, with concentrations similar to those of the completed reaction. Decreasing the stirring rate will tend to stabilize this state at the expense of the high-flow-rate branch. If, in contrast, the induction period is relatively long, isolated regions will tend to be found whose concentrations resemble those of the unreacted input flow—material will be "washed out" of the reactor before it has a chance to react to any significant degree. Decreasing the stirring rate under these conditions will tend to decrease the range of stability of the low-flow-rate branch.

This crude model, which may be thought of as the first in a hierarchy of models that characterize the macromixing process in increasing detail, gives surprisingly good agreement with the experimental results, not only in the chlorite–iodide reaction, but also in systems whose chemistry causes the mixing quality to affect primarily the high-flow-rate rather than the low-flow-rate branch. The branch that is most sensitive to mixing quality and the sequence of bifurcations that occurs as the stirring rate is varied can be accurately predicted, but a quantitative connection between the model parameters on the one hand and the stirring rate and reactor geometry on the other remains elusive. In a real reactor, of course, one does not have two homogeneous zones of different composition, but rather a composition that varies continuously throughout the reactor volume.

A more quantitative picture of the degree of departure from perfect mixing at various stirring rates in the chlorite–iodide reaction was provided by Menzinger and Dutt[14]. They placed a platinum microelectrode at different distances from the central stirring rod in their cylindrical reactor. In one experiment, at a stirring rate of 880 r.p.m., consistent with many experiments on such systems, they observed a difference in electrode potential of about 50 mV when the electrode was moved from a position at the axis to a position 12 mm away in the radial direction. This difference corresponds to a factor of roughly eight in the

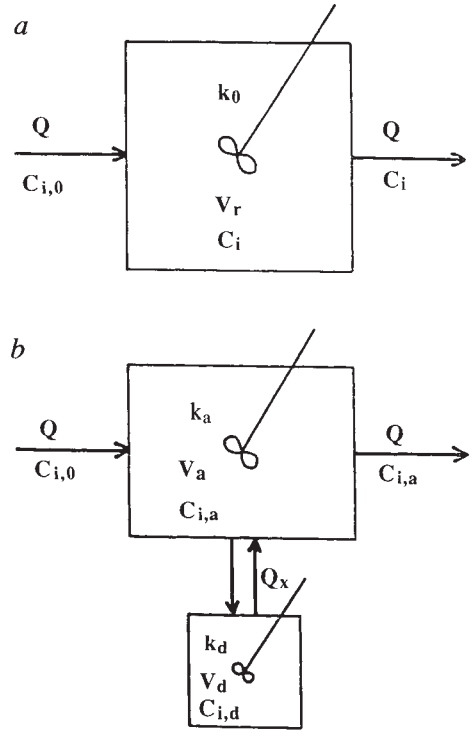

FIG. 2 Two-reactor model[13] of imperfect mixing in a stirred-tank reactor. *a*, Idealized system in which mixing is perfect and concentrations are homogeneous throughout the reactor. *b*, Stirred tank with cross flow between active (well mixed) and dead (poorly mixed) zones. Symbols used: *Q*, volume flow; *C*, concentration; *k*, flow rate (reciprocal residence time); *V*, volume. Subscripts: i, chemical species; o, input from reservoirs; r, homogeneous reactor; a and d, active and dead zones, respectively.

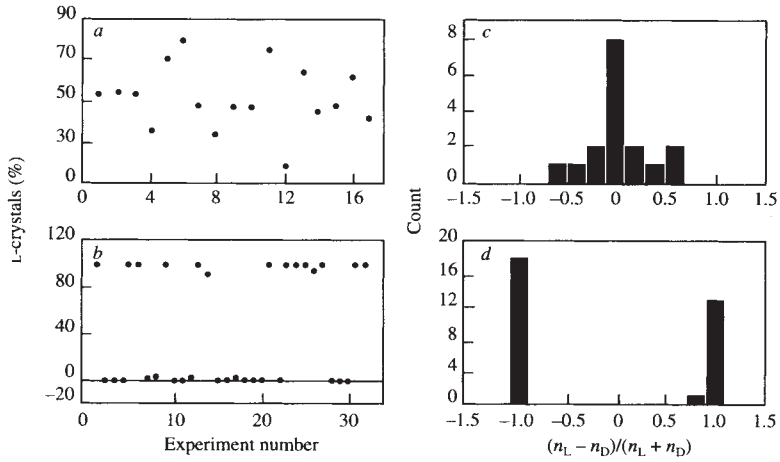

FIG. 3 Statistical analysis of crystallization from stirred and unstirred sodium chlorate solutions[26]. *a*, *b*, Scatter plots of the percentage of L-crystals for unstirred (*a*) and stirred (*b*) experiments. *c*, *d*, Enantiomeric excess of L- over D-crystals in unstirred (*c*) and stirred (*d*) experiments.

iodide concentration! Even at a stirring rate of 2,820 r.p.m., far above the rates normally employed, and very near the threshold for cavitation, $[I^-]$ differed by 17% between the axis of the reactor and the tip of the stirrer.

Some effects of imperfect mixing

Chaos and mixing. The two-reactor model shown in Fig. 2 played a major role in a recent controversy about the origins of chemical chaos in the Belousov–Zhabotinsky (BZ) reaction. Although by the mid-1980s chaotic behaviour had been found experimentally by several groups under a variety of conditions[15–17], no chemically realistic model had been shown to generate chaos. In 1989, Györgyi and Field[18] demonstrated that if the oregonator model[19] for the BZ chemistry was incorporated into a two-reactor model, chaos was easily obtained. They then argued that the experimentally observed chaos arose, not from the inherent (homogeneous) chemical kinetics of the BZ system, but from the coupling of those nonlinear rate laws with imperfect mixing in the experiments.

The Györgyi–Field proposal called into question the source of chaotic behaviour in the best characterized chaotic chemical system. After several months of occasionally heated discussion with experimentalists, Györgyi and Field developed a chemically plausible variant of the oregonator model that produces chaotic behaviour with perfect mixing under conditions resembling those in the experiments[20,21]. Although it remains extremely difficult to pinpoint the origin of chaos in any particular experiment, it now appears that chemical chaos in the BZ reaction can result either from the homogeneous chemistry or from perturbation of that chemistry under periodic oscillating conditions by the effects of imperfect mixing.

Experimental evidence of chaos has since been found in other chemical reactions, such as chlorite–thiosulphate[22], chlorite–thiourea[23] and oxidase–peroxidase[24]. Even where model calculations[25] imply that homogeneous chaos is possible, these systems are as yet too poorly characterized for us to be able to state unambiguously whether or not mixing plays an essential role in the observed chaos.

Chiral symmetry-breaking. Questions about origins, whether of the Universe, of the Earth or of life, have always held great fascination. One intriguing problem of this type is to explain chiral symmetry-breaking in nature; how, for example, it came

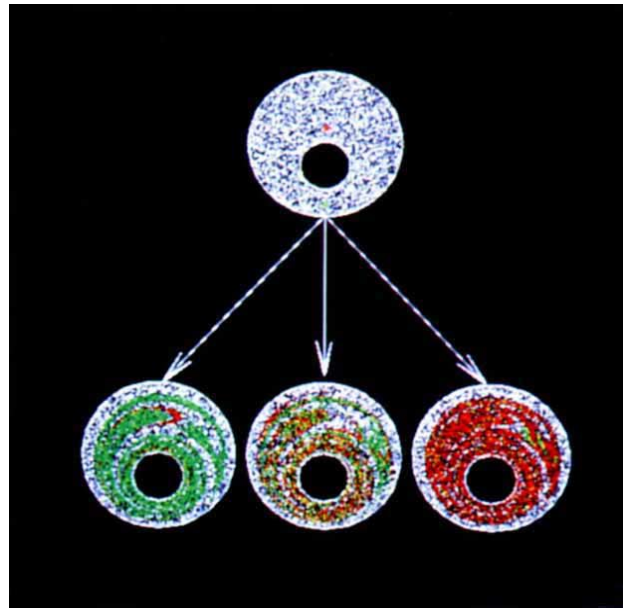

FIG. 4 Simulations of particles in a continuum of solute reacting according to equation (2). The green seed starts at the same location in all three simulations. The initial position of the red seed is moved by 3% to give the three different final states shown in the bottom row. Each simulation starts with 7,000 unreacted white particles, one red and one green seed. With different initial conditions, the flow can produce any final ratio of red to green particles. (By courtesy of G. Metcalfe.)

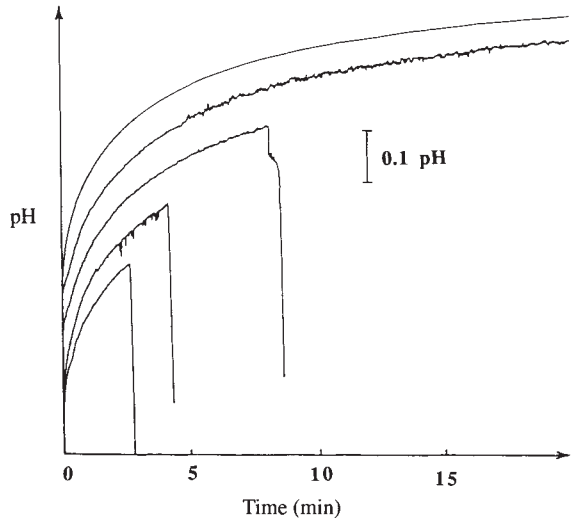

FIG. 5 Representative pH traces in the chlorite–thiosulphate reaction[30] at 20.0 °C measured under identical conditions. Successive curves have been shifted by 0.07 pH units for easier viewing, because in the absence of a shift, the initial portions of the curves coincide nearly perfectly.

to be that nearly all the optically active amino acids of biological significance are laevo- rather than dextro-rotatory. In an experiment that rivals Pasteur's work on optical activity for its simplicity and elegance, Kondepudi *et al.*[26] obtained some remarkable data on the distribution of optical activity among crystals precipitating from a supersaturated solution of sodium chlorate under different mixing conditions. The handedness of the crystals was established visually, using crossed polarizers.

The results are summarized in Fig. 3. When the solution was unstirred, of 1,000 crystals collected from 17 different crystallizations, 525 were of laevo (L) and 475 of dextro (D) chirality; that is, the total numbers were statistically equal, as were the numbers in each individual experiment, as seen in Fig. 3*a* and *c*. When the solution was stirred at 100 r.p.m. during the crystallization process, the total numbers for the 11,829 crystals were consistent with a 50–50 distribution of D- and L-crystals. With only one exception, however, each of the 32 individual crystallizations (Fig. 3*b* and *d*) gave rise to a set of crystals that was more than 99% laevo- or 99% dextro-rotatory!

The authors attribute the observed selectivity to an autocatalytic effect arising from the rapid production of secondary nuclei from a single primary nucleus in the stirred system. In effect, the first "product" particle, the primary nucleus or microcrystal, serves as a chiral template on which further products, the secondary nuclei that grow into crystals, are formed. More recently, Kondepudi and Sabanayagam[27] have demonstrated by scanning electron microscopy that one mechanism of secondary nucleation in sodium chlorate involves the formation and subsequent breaking off by stirring-induced shear forces of needle-shaped structures on primary crystals of sufficient size. They suggest an expression for the rate of secondary nucleation that takes into account the need for the supersaturation, the size of the primary nucleus and the stirring rate all to exceed their threshold values.

Metcalfe and Ottino[28] have modelled the experiments of Kondepudi *et al.*[26] by a simple autocatalytic reaction scheme combined with a chaotic mixing flow. The 'chemistry' is mimicked by a pair of autocatalytic reactions involving white (W), red (R) and green (G) particles:

$$W + G \rightarrow 2G \qquad (2a)$$

$$W + R \rightarrow 2R \qquad (2b)$$

The mixing is approximated by a bounded, two-dimensional, well characterized, Stokes flow characteristic of fluid residing between two parallel but non-concentric cylinders[29]. The simulation is started with a large number of white particles and a single autocatalytic seed particle of each colour. Although the simulations do not lead to 'ultra-high-purity product' of the sort found in the experiments on sodium chlorate crystallization, many initial conditions quickly yield states in which over 90% of the coloured particles are of the same colour (Fig. 4). Perhaps more suggestive of the extreme sensitivity of this system is the fact that very small changes in the initial location of one of the coloured seeds can turn a red-dominated state into a green-dominated one. The authors point to the detailed topology of the mixing, the "highly interwoven nature" of the manifold along which the dominant colour propagates, as the source of this surprising behaviour.

Crazy clocks. Another phenomenon in which autocatalysis and imperfect mixing interact with dramatic effect involves reactions in which there is a sharp transition from an initial, largely unreacted state to the final, equilibrium state. A number of autocatalytic reactions that occur in aqueous solution and that give rise to a colour change serve as the basis for lecture demonstrations known as 'clock reactions'. In a clock reaction, reactant solutions of known concentration are mixed, and there is apparently no reaction until, suddenly, perhaps accompanied by a wave of the hand or magic words from the demonstrator, the solution changes, for example, from red to blue. The time at which the colour change takes place is predictable to very good accuracy (the 'clock' aspect) from a knowledge of the reactant concentrations and the temperature.

In some clock reactions, however, there is a relatively narrow range of concentrations in which the time of this sharp transition becomes essentially unpredictable. The prototype system of this type is the chlorite–thiosulphate reaction[30]. Measurements of pH versus time for five replicate experiments starting from the same initial concentrations are shown in Fig. 5. For the first several minutes, the curves are nearly identical. The pH increases

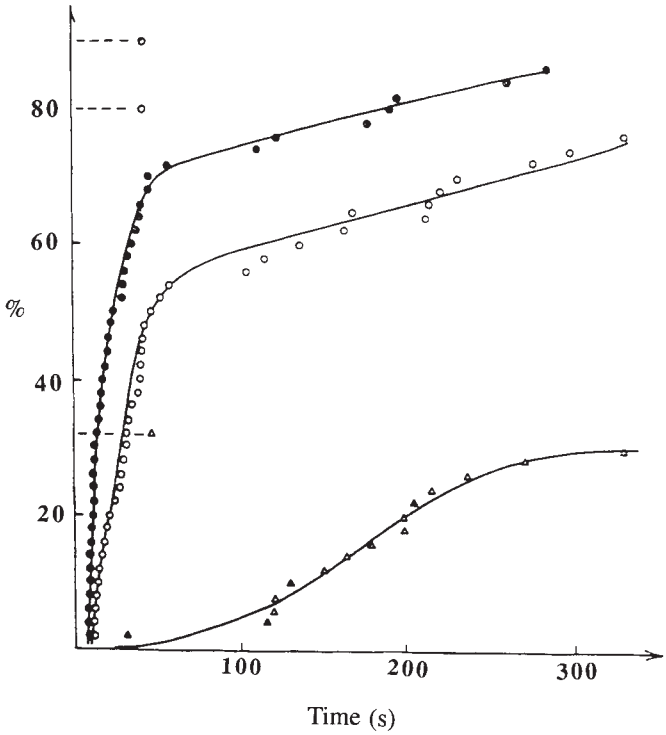

FIG. 6 Percentage of samples reacted as a function of time in the chlorite–thiosulphate reaction for three different stirring rates[30]. Volume, 4.00 cm^3; temperature, 30.0 °C, initial concentration of thiosulphate $[Na_2S_2O_3]_0$, 0.100 M; $[NaClO_2]_0$, 0.300 M; $[NaOH]_0$, 0.100 M. Stirring rate: filled circles (top curve), 500 r.p.m.; open circles (middle curve), 620 r.p.m.; triangles (bottom curve), 700 r.p.m. Note that successive points are equidistant vertically, being separated by 2%, as each distribution is based on 50 measurements.

smoothly. In three of the curves, we observe a sharp drop in pH at approximately 3, 5 and 9 minutes; in the other two, this decrease occurs at times greater than 20 minutes. When an acid–base indicator like phenolphthalein is added to the solution, the pH change is accompanied by a striking colour change. In an 'ordinary' clock reaction, or this same reaction in a different range of reactant concentrations, the sharp pH drop would occur at the same time, to within a few seconds, in all of the curves. What, other than experimental error, might lead to such irreproducibility, sometimes as much as several orders of magnitude, in the reaction times of the anomalous experiments?

Careful efforts to remove all sources of variability among experiments[30] met with total failure. Despite elaborate schemes to ensure that all experiments were the same with regard to temperature, initial concentrations, exposure to light, vessel surface, age of solutions and mixing procedure, the reaction times still varied over a wide range. The distribution of reaction times for, say, a set of 100 replicate experiments under the same conditions was, however, statistically reproducible. If the conditions such as reactant concentrations, temperature, stirring rate or, most remarkably, the volume of the vessel, were varied, the distribution of reaction times changed significantly. In Fig. 6, I show a cumulative probability distribution of reaction times for three sets of experiments carried out with three different stirring rates. In these experiments, both the mean and the standard deviation of the reaction-time distribution increase as the stirring rate increases or as the reaction volume decreases.

Mechanistic analysis of the chlorite–thiosulphate reaction as well as consideration of the reaction-time distributions led to the following qualitative explanation for the observed behaviour. The pH rise and subsequent drop result from competition between two reaction pathways starting from chlorite and thiosulphate:

$$4S_2O_3^{2-} + ClO_2^- + 4H^+ \rightarrow 2S_4O_6^{2-} + 2H_2O + Cl^- \quad (3)$$

$$S_2O_3^{2-} + 2ClO_2^- + H_2O \rightarrow 2SO_4^{2-} + 2H^+ + 2Cl^- \quad (4)$$

Reaction (3) is responsible for the initial pH rise; its rate is proportional to $[H^+]$. Reaction (4) accounts for the pH drop. It is 'supercatalytic', with a rate proportional to $[H^+]^2[Cl^-]$. In the bulk of the solution, reaction (3) is the dominant pathway. However, if in some small region a fluctuation leads to a sufficiently high concentration of hydrogen ions, the autocatalysis in reaction (4) can produce a rapid local build-up of $[H^+]$, which spreads through the solution, causing the observed rapid pH drop.

The stochastic nature of the reaction-time distribution results from the fact that these supercritical concentration fluctuations are rare, random events. The observed effects of stirring and volume on the distribution support this interpretation. By increasing the effectiveness of the mixing, one decreases the likelihood that any given fluctuation will grow to critical size before it is dissipated by mixing with the high-pH bulk. Note that if the stirring is stopped at any time after the first few seconds, all samples react completely within three seconds. The more puzzling volume effect can be understood simply in terms of the number of possible microvolumes within the sample in which a supercritical fluctuation can occur. The larger the volume of the system, the more likely such a fluctuation and the shorter the mean reaction time.

Although the behaviour described above is rare, it is by no means unique to the chlorite–thiosulphate reaction. Similar distributions of reaction times are found in the chlorite–iodide reaction[31] in a concentration range where it shows high-order autocatalysis. Ferrone *et al.*[32] and Hofrichter[33] have observed a stochastic variation in the distribution of times at which polymerizing sickle haemoglobin molecules undergo a sharp transition from the monomeric to the polymeric state. They suggest a route involving a highly autocatalytic "double nucleation" mechanism that shares important features with the scheme outlined above for the chlorite–thiosulphate reaction and with Kondepudi's description of secondary nucleation in sodium chlorate crystallization. The primary nucleus is a polymer of sickle haemoglobin that exceeds a critical length, beyond which it can serve as a template for the formation of new polymer chains.

Lemarchand *et al.*[34] reported a stochastic distribution of ignition times in experiments on the kinetics of cool flames in mixtures of *n*-pentane and air. Combustion reactions tend to be poorly mixed, because of the complex spatial structure of flames, and autocatalytic, both because of the occurrence of radical chain reactions and because the reaction rates increase as the temperature rises.

At least two theoretical approaches provide a more quantitative account of these stochastic reaction-time distributions. Szabo[35] has used the theory of first passage times and a simple birth and death model to obtain an analytical expression that is in good agreement with the sickle haemoglobin polymerization results. Sagués *et al.*[36] use a more detailed chemical model with noise terms incorporated through the kinetic constants to simulate the reaction-time distributions in experiments on the chlorite–iodide reaction. In both cases, mixing efficiency serves as a parameter: in the Szabo approach it determines the initial nucleation probability; in the noise-term method the intensity of the noise is empirically correlated with the stirring rate.

Conclusion

The past decade has witnessed a growing understanding of the rich variety of behaviour of which nonlinear, and especially autocatalytic, chemical reactions are capable. Typically, more complex behaviour emerges when a control parameter such as the temperature or a reactant concentration is varied past a critical value. The studies described here suggest that mixing effectiveness, difficult though it may be to quantify, can serve as an additional, more subtle control parameter. In addition, the interaction of mixing with autocatalysis can give rise to new phenomena such as chiral symmetry-breaking and stochastic behaviour. As we have seen, the interaction of autocatalysis and mixing gives rise to interesting effects in both open and closed systems.

From a theoretical point of view, the extreme cases of perfectly mixed, homogeneous systems and of unmixed, diffusive systems are far better understood than the intermediate case of partially mixed systems, though the latter are far more common in nature. An accurate description of the mixing process is still far beyond our current theoretical capabilities, but, as some of our examples show, even a rather crude model of the mixing when coupled to a reasonable chemical scheme can yield insight into many of the phenomena of interest.

Further study of the behaviour that can arise in imperfectly mixed autocatalytic systems should prove rewarding. There may well be new phenomena to be discovered. The notion of tuning the mixing efficiency to control the composition of the output from an industrial reactor is an appealing potential extension of the experiments that produce chirally pure sodium chlorate crystals. Workers at duPont (Roelofs and Wasserman, unpublished observations) have studied the oxidation of toluene in an effort to gain insight into the analogous *p*-xylene oxidation reaction that generates the starting material for polyester fibre. The reaction is autocatalytic and oscillatory. In a large reactor similar to those employed industrially, the phase and amplitude of the oscillations vary from place to place in the reactor. This variation can be reduced, although not totally eliminated, by increasing the rate at which the solution is stirred. The consequences of this spatial inhomogeneity for the yield and purity of the product are not yet known, but seem worth exploring further.

Finally, the possible consequences of imperfect mixing in living systems merit additional scrutiny. As noted at the outset, population growth is an inherently autocatalytic process. In a

BOX 1 A simple population-dynamics example

Consider a set of species with populations p_1, p_2, ... Assume that each grows and dies at rates proportional to its population,

$$dp_i/dt = (b_i - d_i)p_i = r_i p_i \quad (5)$$

where b_i and d_i are the *per capita* birth and death rates, respectively, and r_i is the net *per capita* growth rate of the ith species. If the food supply is unlimited and if there are no (for example, predator–prey) interactions between species, then all populations grow exponentially, and the species with the largest growth rate r_i will eventually come to dominate the population regardless of the initial populations p_{i0}. A similar conclusion holds for any other growth law if the growth is unconstrained.

In some cases, for example that of equation (1), one may wish to take the effects of a limited food supply or other environmental constraints into account by making the growth rate a nonlinear function of the population. Alternatively, one might include these effects by constraining the total population. We can maintain the total population, $P = \sum p_i$, constant by adding a flux term to our population growth equation. The particular form of the constraint used in equations (6*a*) and (6*b*) below for a pair of competing species is referred to by Eigen and Schuster[37] in their models of molecular evolution as the constraint of constant organization. With initial populations p_{10} and $p_{20} = P - p_{10}$, the growth equations are

$$dp_1/dt = r_1 p_1 - (p_1/P)(r_1 p_1 + r_2 p_2) \quad (6a)$$

$$dp_2/dt = r_2 p_2 - (p_2/P)(r_2 p_2 + r_1 p_1) \quad (6b)$$

Note that $dp_1/dt + dp_2/dt = 0$. Because $p_2 = P - p_1$, we can eliminate p_2 from equation (6*a*) to obtain a single growth equation for p_1:

$$dp_1/dt = r_1 p_1 - (p_1/P)[r_1 p_1 + r_2(P - p_1)]$$

$$= [(r_2 - r_1)/P][p_1(p_1 - P)] \quad (7)$$

Equation (7) can be solved exactly for $p_1(t)$ to yield

$$p_1(t) = P/[1 - (1 - P/p_{10}) \exp[(r_2 - r_1)t]] \quad (8)$$

As $t \to \infty$ our expression for $p_1(t)$ approaches 0 if $r_2 > r_1$; it approaches P if $r_2 < r_1$. We thus have all-or-none selection of the faster growing species, independent of the initial populations, so long as neither starts at zero.

Now consider a pair of species evolving with a nonlinear growth rate, say quadratic, again under the constraint of constant organization. The evolution equations for this system take the form

$$dp_1/dt = r_1 p_1^2 - (p_1/P)(r_1 p_1^2 + r_2 p_2^2) \quad (9a)$$

$$dp_2/dt = r_2 p_2^2 - (p_2/P)(r_1 p_1^2 + r_2 p_2^2) \quad (9b)$$

Substitution of $P - p_1$ for p_2 in equation (9*a*) yields, after some algebraic manipulation,

$$dp_1/dt = -[(r_1 + r_2)/P]p_1[p_1 - r_2 P/(r_1 + r_2)](p_1 - P) \quad (10)$$

Equation (10) can be solved exactly for $p_1(t)$, but a graphical solution is more revealing. In the box figure, I have plotted dp_1/dt versus p_1: the arrows show the direction in which the system evolves. From the sign of the time derivative, we see that if p_1 is initially less than $p' = r_2 P/(r_1 + r_2)$ it will decrease until it reaches a final value of zero, that is, species 1 will die out. If $p_1 > p'$, then it will grow until it reaches P. We again have all-or-none selection, but now the winner of the battle depends, not simply on the growth rate, but on whether or not p_1 initially exceeds p'. Survival of the fittest is no longer the operative principle; it matters who gets in first. Note that

$$p' = r_2 P/(r_1 + r_2) = r_2(p_1 + p_2)/(r_1 + r_2)$$

so that the condition $p_1 > p'$ is equivalent to $p_1(r_1 + r_2) > r_2(p_1 + p_2)$, or equivalently, to $r_1 p_1 > r_2 p_2$. Selection that is dependent on the initial conditions occurs for any growth law that exceeds linearity in its dependence on the populations. Similar conclusions can be reached for an arbitrary number of species[37].

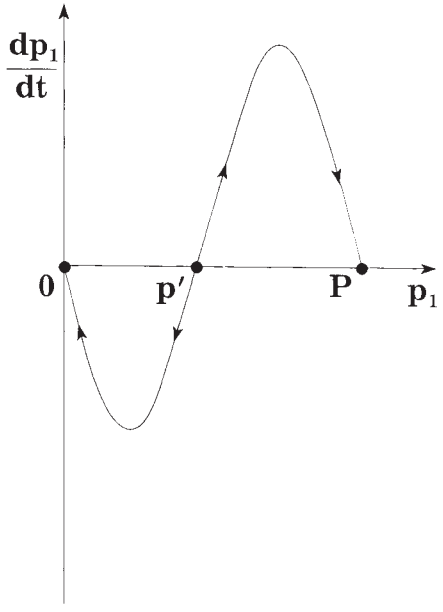

perfectly mixed system of species competing for a common, fixed food supply, there will be all-or-none selection (see Box 1). The situation resembles somewhat the L- and D-crystals competing for the dissolved sodium chlorate in the experiments of Kondepudi *et al.*[26].

The "fittest" species will ultimately win out as shown in Box 1. The definition of fitness varies with the rate law for reproduction and the environment in which the competition takes place. If the food supply is unlimited or if the growth rate is linear, even a single reproductively capable individual will give rise to descendants who will dominate an established population of lower fecundity (or survivability). If the food supply is limited and the growth rate is nonlinear, then history plays a role. In order to win the competition, a new species must first reach a certain population threshold at which its absolute, not its relative rate of reproduction is the largest in the system. For species with quadratic growth rates r_1 and r_2 and populations p_1 and p_2, this means that species 1 will be the final survivor if and only if p_1 initially exceeds $(r_2/r_1)p_2$. In effect, a favourable mutation cannot survive unless there is a way for its population to reach a critical level before it is swamped by competition from its less able but more populous neighbours.

One way in which real entities avoid the wastefulness of all-or-none selection is through less-than-perfect mixing. Mobile organisms can isolate themselves from direct competition with their better adapted fellows by spatially segregating themselves, by choosing a niche. Darwin recognized that more exotic, though perhaps 'less fit' species were likely to be found in isolated habitats such as islands. Eigen and Schuster[37] have considered a model of the earliest self-reproducing macomolecules forming from their monomeric components in a puddle of primaeval broth. They find that, to the extent that different molecules can find different puddles in which to grow, or that compartmentalization can arise from the development of primitive cell membranes, the mixture will be able to support a richer variety of complex species. Kareiva and Wennergren[38] have recently reviewed the fascinating literature on how landscape patterns and species mobility affect population dynamics in complex ecological systems. Again, the rates at which species mix and spread are found to have dramatic effects on the behaviour of the system.

Whether the sorts of experiments described here will give us further insight into controlling the outputs of vats of industrially important chemicals or will allow us to understand better the mysteries of molecular or species evolution remains to be seen. What is already clear is that the interaction of autocatalytic

processes with imperfect mixing leads to a rich variety of phenomena and that there is still much to be learned about the behaviour of such systems. □

Irving R. Epstein is at the Department of Chemistry and Volen Center for Complex Systems, Brandeis University, Waltham, Massachusetts 02254-9110, USA.

1. May, R. M. *Nature* **261,** 459–467 (1976).
2. Jahnke, W. & Winfree, A. T. *J. chem. Educ.* **68,** 320–324 (1991).
3. Devreotes, P., Fontana, D., Klein, P., Sherring J. & Theibert A. *Meth. Cell. Biol.* **28,** 299–331 (1987).
4. Lechleiter, J., Girard, S. E., Peralta, E. G. & Clapham, D. *Science* **252,** 123–126 (1991).
5. Turing, A. M. *Phil. Trans. R. Soc.* B**237,** 37–72 (1952).
6. Castets, V., Dulos, E., Boissonade, J. & De Kepper, P. *Phys. Rev. Lett.* **64,** 2953–2956 (1990).
7. Malthus, T. R. *An Essay on the Principle of Population* 14 (Oxford Univ. Press, London, 1798).
8. Epstein, I. R. *J. chem. Educ.* **66,** 191–195 (1989).
9. Villermaux, J. *Rev. chem. Engng.* **7,** 51–108 (1991).
10. Roux, J. C., De Kepper, P. & Boissonade, J. *J. Phys.* **97A,** L168–L170 (1983).
11. De Kepper, P., Boissonade, J. & Epstein, I. R. *J. phys. Chem.* **94,** 6525–6536 (1990).
12. Luo, Y. & Epstein, I. R. *J. chem. Phys.* **85,** 5733–5740 (1986).
13. Kumpinsky, E. & Epstein, I. R. *J. chem. Phys.* **82,** 53–57 (1985).
14. Menzinger, M. & Dutt, A. K. *J. phys. Chem.* **94,** 4510–4514 (1990).
15. Schmitz, R. A., Graziani, K. R. & Hudson, J. L. *J. chem. Phys.* **67,** 3040–3044 (1977).
16. Roux, J. C., Rossi, A., Bachelart, S. & Vidal, C. *Phys. Lett.* A**77,** 391–393 (1980).
17. Roux, J. C., Simoyi, R. H. & Swinney, H. L. *Physica* D**8,** 257–266 (1983).
18. Györgyi, L. & Field, R. J. *J. chem. Phys.* **91,** 6131–6141 (1989).
19. Field, R. J. & Noyes, R. M. *J. chem. Phys.* **60,** 1877 (1974).
20. Györgyi, L. & Field, R. J. *J. phys. Chem.* **95,** 6594–6602 (1991).
21. Györgyi, L. & Field, R. J. *Nature* **355,** 808–810 (1992).
22. Maselko, J. & Epstein, I. R. *J. chem. Phys.* **80,** 3175–3178 (1984).
23. Alamgir, M. & Epstein, I. R. *Int. J. chem. Kinet.* **17,** 429–439 (1985).
24. Olsen, L. F. & Degn, H. *Nature* **267,** 177–178 (1977).
25. Aguda, B. D. & Larter, R. *J. Am. chem. Soc.* **113,** 7913–7916 (1991).
26. Kondepudi, D. K., Kaufman, R. J. & Singh, N. *Science* **250,** 975–976 (1990).
27. Kondepudi, D. K. & Sabanayagam, C. *Chem. Phys. Lett.* **217,** 364–368 (1994).
28. Metcalfe, G. & Ottino, J. M. *Phys. Rev. Lett.* **72,** 2875–2878 (1994).
29. Swanson, P. D. & Ottino, J. M. *J. Fluid Mech.* **213,** 227–249 (1990).
30. Nagypál, I. & Epstein, I. R. *J. phys. Chem.* **90,** 6285–6292 (1986).
31. Nagypál, I. & Epstein, I. R. *J. chem. Phys.* **89,** 6925–6928 (1988).
32. Ferrone, F. A., Hofrichter, J. & Eaton, W. A. *J. molec. Biol.* **183,** 591–610, 611–631 (1985).
33. Hofrichter, J. *J. molec. Biol.* **189,** 533–571 (1986).
34. Lemarchand, A., Ben Aim, R. I. & Nicolis, G. *Chem. Phys. Lett.* **162,** 92–98 (1989).
35. Szabo, A. *J. molec. Biol.* **199,** 539–542 (1988).
36. Sagués, F., Ramirez-Piscina, L. & Sancho, J. M. *J. chem. Phys.* **92,** 4786–4792 (1990).
37. Eigen, M. & Schuster, P. *The Hypercycle. A Principle of Natural Self-Organization* (Springer, Berlin, 1979).
38. Kareiva, P. & Wennergren, U. *Nature* (in the press).

ACKNOWLEDGEMENTS. I thank K. Kustin, R. Field and J. Pojman for helpful discussions. This work was supported by the US NSF.

Structural basis of cell–cell adhesion by cadherins

Lawrence Shapiro*, Allison M. Fannon†, Peter D. Kwong*, Andrew Thompson‡, Mogens S. Lehmann§‖, Gerhard Grübel§, Jean-François Legrand§¶, Jens Als-Nielsen§¶, David R. Colman† & Wayne A. Hendrickson*#

* Department of Biochemistry and Molecular Biophysics, and # Howard Hughes Medical Institute, Columbia University, New York, New York 10032, USA
† Brookdale Center for Molecular Biology, Mount Sinai School of Medicine, New York, New York 10029, USA
‡ European Molecular Biology Laboratory, BP 156 X, 38042 Grenoble, France
§ European Synchrotron Radiation Facility, BP 220, 38043 Grenoble, France
‖ Institut Laue Langevin, BP 156 X, 38042 Grenoble, France

Crystal structures of the amino-terminal domain of N-cadherin provide a picture at the atomic level of a specific adhesive contact between cells. A repeated set of dimer interfaces is common to the structure in three lattices. These interactions combine to form a linear zipper of molecules that mirrors the linear structure of the intracellular filaments with which cadherins associate. This cell-adhesion zipper may provide a mechanism to marshal individual molecular adhesive interactions into strong bonds between cells.

MANY cells of multicellular organisms are able to distinguish different cell types, generally adhering preferentially to cells of their own type[1,2]. This selective cell adhesion, which arises as the result of expression of specific adhesive molecules on the cell surface, is fundamental to controlling the development and maintenance of tissues. The cadherin family of cell–cell adhesion receptors, whose members are expressed widely in the solid tissues of both vertebrates and invertebrates[3], is central to this process[4]. N-cadherin[5,6], which first appears in the vertebrate nervous system during formation of the neural tube, functions in morphogenesis and homeostasis in the nervous system and other tissues[7].

Cadherins are transmembrane glycoproteins characterized by a distinctive sequence motif which is tandemly repeated in their extracellular segments[5]. We show here that these repeated sequences form autonomously folded protein modules ('cadherin domains'). Each cadherin subtype has a unique, usually homophilic, binding specificity that confers specific cell-adhesive properties on the cells in which it is expressed[8]. Experiments with molecular chimaeras[6], neutralizing antibodies[9] and peptide inhibitors[10] suggest that the binding specificity resides in the first (N-terminal) cadherin domain.

The adhesive action of cadherins is dependent on the presence of extracellular Ca^{2+} ions[11], and it has long been known that Ca^{2+} affords substantial protection against exogenous proteases[12]. Intracellular domains of cadherins mediate connections

¶ Permanent addresses: Laboratoire de Spectrométrie Physique (URA CNRS no. 8), Université J. Fourier-Grenoble 1, BP 87, 38402 Saint Martin d'Hères Cedex, France (J.-F.L.); Risø National Laboratory, DK 4000 Roskilde, Denmark (J.A.-N.).